Learning Imaging

Series Editors:

R. Ribes · A. Luna · P.R. Ros

Joan C. Vilanova · Antonio Luna
Pablo R. Ros
(Editors)

Learning Genitourinary and Pelvic Imaging

Springer

Joan C. Vilanova
Clinica Girona
Dept. Magnetic Resonance
Lorenzana 36
17002 Gerona
Spain
kvilanova@comg.cat

Antonio Luna
Clinica Las Nieves Sercosa
Carmelo Torres 2
23007 Jaén
Spain
aluna70@sercosa.com

Pablo R. Ros
Case Western Reserve University
Dept. Radiology
Bolwell B124
Euclid Ave. 11100
44106 Cleveland Ohio
USA
pablo.ros@uhhospitals.org

ISBN: 978-3-642-23531-3 e-ISBN: 978-3-642-23532-0

DOI: 10.1007/978-3-642-23532-0

Springer Heidelberg Dordrecht London New York

Library of Congress Control Number: 2011940863

Printed on acid-free paper

9 8 7 6 5 4 3 2 1

Springer is part of Springer Science+Business Media (www.springer.com)

Contents

Contributors

Ignacio Alvarez Rey
Servicio de Radiodiagnóstico
Xanit Hospital Internacional
Benalmádena
Málaga
Spain

Joaquim Barceló
Department of Radiology
Clínica Girona-Hospital Sta. Caterina
University of Girona
Girona
Spain

Sandra Baleato
Department of Radiology
CHUS Complexo Hositalario Universitario de Santiago
Coruña
Spain

Maria Boada
Department of Radiology
Clínica Girona
Girona
Spain

Laura Buñesch
Department of Radiodiagnostic
Imaging Center
Hospital Clínic
Barcelona
Spain

Iria Couto Rodríguez
Department of Radiology
Complexo Hospitalario Universitario de Santiago de Compostela
Santiago de Compostela
Spain

Gabriel C Fernández
Department of Radiology
HNSS (Hospital Nuestra Señora de Sonsoles)
Ávila
Spain

Roberto García-Figueiras
Department of Radiology
Complexo Hospitalario Universitario de Santiago de Compostela
Santiago de Compostela
Spain

Guadalupe Garrido
Diagnostic Imaging Department
Hospital Clínico
Málaga
Spain

Antonio Luna
Clinica Las Nieves Sercosa
Jaén
Spain

Teodoro Martín Noguerol
Clinica Las Nieves, Sercosa
Jaén
Spain

Carlos Nicolau
Department of Radiodiagnostic
Imaging Center
Hospital Clínic
Barcelona
Spain

Rafael Oliveira Cafaia
Radiology Department
Hospital Clínic
Barcelona
Spain

Blanca Paño Brufau
Radiology Department
Hospital Clínic
Barcelona
Spain

María Pérez Alarcón
Department of Radiology
Complexo Hospitalario Universitario de Santiago de Compostela
Santiago de Compostela
Spain

Marcelo Potolicchio
Ultrasound Unit
DADISA
Cádiz
Spain

Rafael Salvador Izquierdo
Radiology Department
Hospital Clínic
Barcelona
Spain

Carmen Sebastià
Department of Radiodiagnostic
Imaging Center
Hospital Clínic
Barcelona
Spain

Joan C. Vilanova
Department of Radiology
Clínica Girona-Hospital Sta. Caterina
Gerona
Spain

Mariano Volpacchio
Centro diagnóstico Rossi
Buenos Aires
Argentina

Kidney 1

Carlos Nicolau, Carmen Sebastià, and Blanca Paño Brufau

Contents

J.C. Vilanova et al. (eds.), *Learning Genitourinary and Pelvic Imaging*, Learning Imaging,
DOI 10.1007/978-3-642-23532-0_1, © Springer-Verlag Berlin Heidelberg 2012

Case 1

Bilateral Renal Artery Fibromuscular Dysplasia

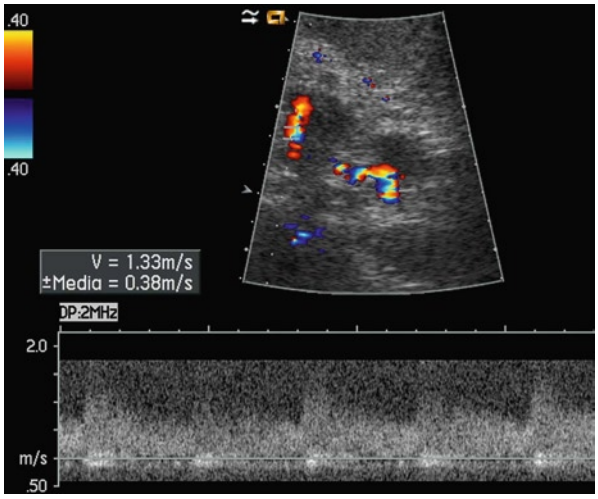

Fig. 1.1

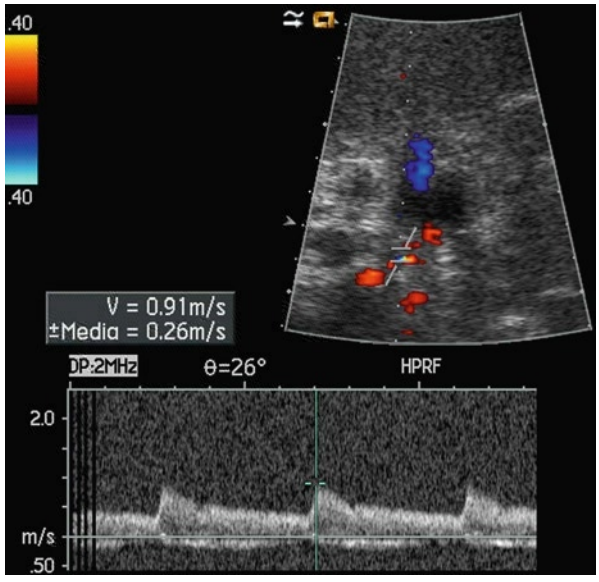

Fig. 1.2

Fig. 1.3

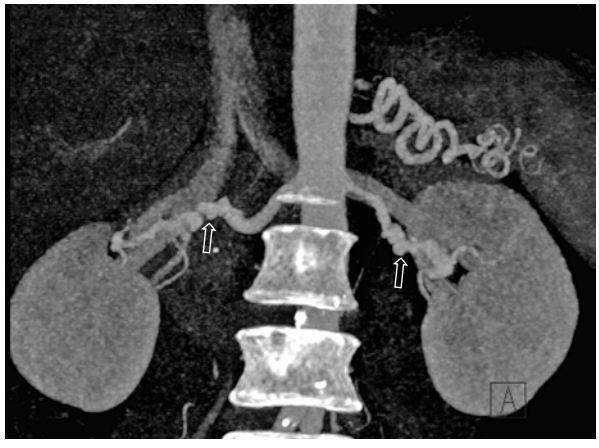

Fig. 1.4

A 54-year-old man presented to the emergency room with a hypertensive crisis and was successfully treated with antihypertensive treatment. A renal artery Doppler ultrasound was performed as part of the evaluation of the hypertension.

Comments

Fibromuscular dysplasia (FMD) is a non-atherosclerotic, non-inflammatory vascular disease that affects medium- and large-sized arteries, most commonly the renal and internal carotid arteries, but has been described in almost every arterial bed in the body. Clinical presentation may vary from an asymptomatic condition to a multisystem disease that mimics necrotizing vasculitis. It is known to be the second major cause of renovascular hypertension, atherosclerosis being the leading cause. Renovascular FMD tends to affect young women with no cardiovascular risk factors. Asymptomatic FMD is a finding that appears in 2–6% of multi-detector computed tomography (MDCT) scans of living renal donors, who are considered a sample of healthy people. In two-thirds of symptomatic patients, renal artery FMD is bilateral. Little is known about the long-term progression of asymptomatic FMD that is discovered incidentally. Duplex ultrasound imaging can accurately detect elevated blood-flow velocities in the middle to distal portion of the main renal arteries or segmental arteries. If the areas of stenosis are hemodynamically significant, a parvus-tardus waveform is seen on Doppler ultrasound in the intrarenal arteries. CT findings of FMD are very characteristic and show a "string-of-beads" or beaded appearance or focal stenosis or aneurysms usually in the mid- or distal main renal artery and the segmental renal arteries. If MDCT findings of FMD are clear, we can accurately diagnose the condition with this technique. In case of doubt, an angiography is mandatory.

Because of its better spatial resolution and the subtle findings of FMD, MDCT is preferred over MR for diagnosis. It is not difficult to differentiate FMD from renal artery atherosclerosis since the latter occurs at the origin or proximal artery in older patients with typical cardiovascular risk factors. If the medical treatment fails, percutaneous transluminal angioplasty or surgical revascularization are the primary therapeutic options.

Imaging Findings

Doppler ultrasound of the right artery shows increased flow of the distal right main renal artery (1.3 m/seg) compared to the proximal right main renal artery (0.9 m/seg) (Figs. 1.1 and 1.2). Doppler ultrasound shows decreased initial acceleration in intrarenal arteries consistent with the parvus-tardus waveform (not shown). Due to the suspicious findings of right main renal artery stenosis on Doppler ultrasound examination, an angio-CT was performed. Thin-MIP reformatted images in axial and coronal views (Figs. 1.3 and 1.4) show typical beading of the middle to distal portion of both renal arteries ("string of beads" appearance), suggestive of renal artery FMD (arrows). Note that the proximal renal arteries are not affected.

Case 2

Active Multifocal Bleeding of the Renal Capsular Branches Secondary to Subcapsular Hematoma

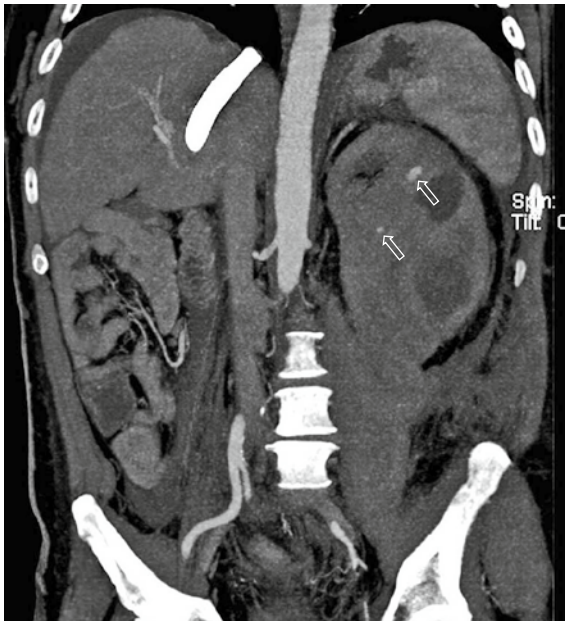

Fig. 1.5

Fig. 1.6

Fig. 1.7

Fig. 1.8

A 48-year-old man with antiphospholipid syndrome and Budd-Chiari syndrome was admitted to the hospital for a renal biopsy to diagnose the sudden impairment of renal function. No complications appeared during the left renal biopsy and the patient was discharged the following day. Fifteen days after the biopsy and coinciding with the day the patient restarted the anticoagulant therapy, he complained of left flank pain and went to the emergency room. Laboratory tests showed a severely low red blood cell count. CT and angiography showed multifocal active bleeding on the renal surface from a subcapsular hematoma. Multiple partial embolizations of the left kidney were successfully performed and the patient was discharged 10 days later with a renal function of 30%.

Comments

Multifocal bleeding from ruptured capsular branches is an extremely rare condition; only two cases have been reported in the English literature. This condition usually appears after aggressive procedures on the kidneys (nephrostomy, stent placement or biopsy), with increased frequency in atrophic kidneys or in patients on anticoagulant therapy. It is believed that this traumatic procedure leads to subcapsular hematoma formation that causes rupture of the capsular arteries with multiple focal active bleeding. CT depicts a non-enhanced hyperdense subcapsular collection that compresses the kidney with multiple small focus of active bleeding inside the hematoma. Angiography shows multiple areas of perirenal arterial extravasation or pseudoaneurysms formation. Differential diagnosis with aneurysms secondary to vasculitis is required. These aneurysms occur in the intrarenal arterial branches whereas capsular pseudoaneurysms occur on the renal surface. The treatment of choice is angiographic embolization or nephrectomy. Usually an important loss of renal function appears after embolization secondary to the multiple bleeding sites.

Imaging Findings

Arterial enhanced coronal and axial CT scans (Figs. 1.5–1.7) show compressed kidney by a severe subcapsular hematoma. Multiple small foci of active arterial bleeding are seen inside the hematoma near the kidney surface (arrows in Figs. 1.6 and 1.7). Selective angiography of the left renal artery demonstrates multiple small pseudoaneurysms in the kidney surface consistent with active bleeding of the capsular arteries (Fig. 1.8).

Case 3
Pyelonephritis

A 55-year-old diabetic woman presents with a 7-day history of bilateral flank pain, fever of 39°C, nausea and vomiting.

Comments

In adults, diagnosis of urinary tract infection is typically based on characteristic clinical features and abnormal laboratory values.

Imaging should, in general, be reserved for those patients in whom conventional treatment has failed.

Ultrasonography (US)

It is important to be aware of the US findings because sometimes they are subtle. US is limited in the identification of perinephric extension of infection, and in the visualization of small microabscesses.

Fig. 1.9

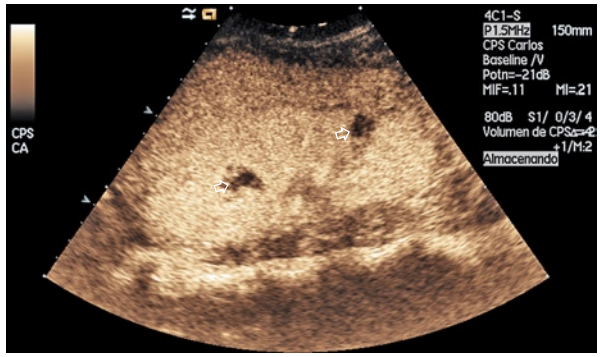

Fig. 1.11

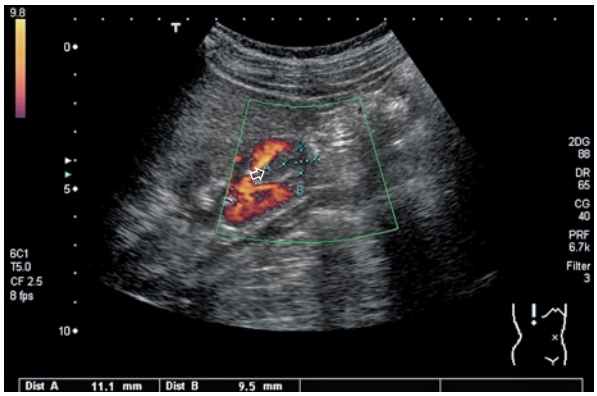

Fig. 1.10

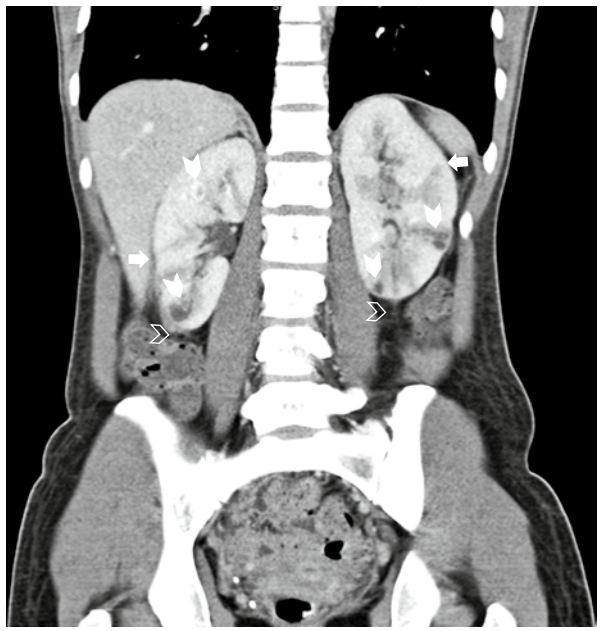

Fig. 1.12

Doppler evaluation typically demonstrates decreased perfusion in the affected parenchyma. Power Doppler is superior to color Doppler in defining the extent of hypoperfusion. However, Doppler evaluation is limited in the detection of low flow and flow in small vessels.

The advent of US contrast agents improves sensitivity of US in defining the extent of hypoperfusion.

Computed Tomography (CT)

CT is the modality of choice for evaluating acute pyelonephritis. According to the Society of Uroradiology, all regions of hypoattenuating parenchyma on CT should be considered acute pyelonephritis and the disease should be described in terms of uni/bilateral, focal/diffuse, focal swelling/no-focal swelling or renal enlargement/no-renal enlargement.

A reasonable renal infection CT protocol should include precontrast followed by postcontrast imaging at nephrographic phase, and include the excretory phase only if urinary obstruction is suspected.

Unenhanced CT can detect obstruction, calculi, gas formation, hemorrhage, parenchymal calcifications, renal enlargement and inflammatory. Perinephric stranding alone should be interpreted with caution as even in presence of acute symptomatology, it may relate to previous infection, trauma or vascular disease.

At excretory phase, soft tissue filling defects in the collecting system may be present corresponding to blood clots, inflammatory debris or sloughed tissue from papillary necrosis.

Typical features at US/CT include:

1. Focal or global enlargement of the kidney, sometimes with a mass-like appearance.
2. Ill-defined, wedged-shaped area of hypoechoic/decreased attenuation radiating from the papilla to the cortical surface. Differential diagnosis includes areas of focal infarction, tumors or scarring.
3. At CT, striated nephrogram, seen as linear bands of alternating hyper and hypoattenuation orientated parallel to the axes of the tubules and collecting ducts. Striations are not pathognomonic of acute pyelonephritis.
4. Loss of corticomedullary differentiation at US.
5. Obliteration of the renal sinus and perinephric fat planes, stranding, thickening of Gerota's fascia at CT.
6. Thickening of the pelvicalyceal wall.
7. Microabscesses are identified as hypoechoic mass that lacks internal flow on color Doppler images at US, or non-enhancing fluid collections within abnormal areas of parenchyma that may have an enhancing rim. Abscess cavities may be large and require drainage in some cases.
8. Hydronephrosis/pyonephrosis.

Radiological Findings

US (Fig. 1.9) image shows right global enlarged kidney with several cortical hypoechoic round areas with ill-defined margins (open arrows). Power Doppler US evaluation (Fig. 1.10) and especially contrast-enhanced US (Fig. 1.11) improve the sensitivity to parenchyma abnormalities and demonstrate decreased perfusion in the affected parenchyma (arrows). CT in nephrographic phase (Fig. 1.12) shows bilateral renal enlargement, striated nephrogram (arrows) and peripheral fat stranding (open arrowhead). Ill-defined, non-enhancing fluid collections (microabscesses) within abnormal areas of parenchyma radiating from the papilla (arrowheads) are seen.

Case 4

Peritoneal Seeding of Xanthogranulomatous Pyelonephritis

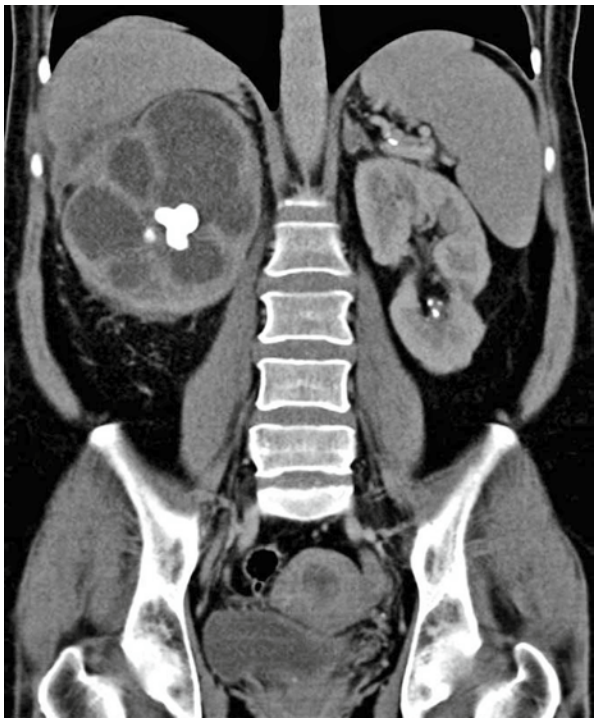

Fig. 1.13

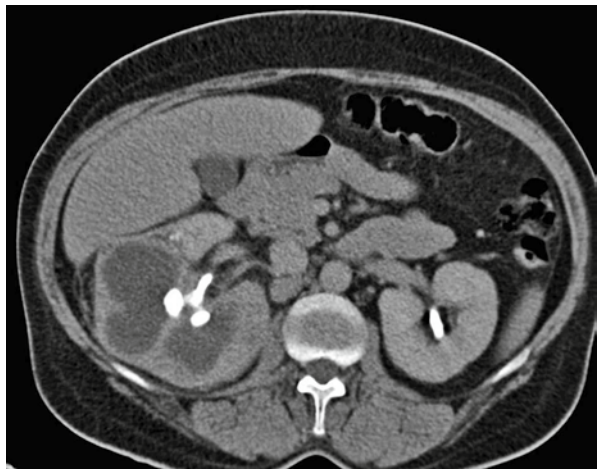

Fig. 1.14

Fig. 1.15

Fig. 1.16

A 57-year-old woman was admitted to the emergency room complaining of fever and lumbar pain. Laboratory tests showed infection parameters. Abdominal ultrasound (US) and computed tomography (CT) were performed. Laparoscopic right nephrectomy was done; during surgery right kidney and peritoneum were accidentally opened. Five days later, the patient had no complications and was discharged. Six months later, he complained of pelvic pain with no other symptoms, and transvaginal US and CT were performed.

Comments

Xanthogranulomatous pyelonephritis (XP) is an uncommon reaction of the kidney to chronic infection in the setting of chronic obstruction. Diabetes mellitus is seen in 10% of these patients. The most common organisms involved are *P. mirabilis* and *E. coli*. Renal parenchyma is replaced by granulation tissue containing lipid-laden macrophages. Most cases occur in association with a renal pelvic calculus; hydronephrosis is thought to be a contributing factor. Symptoms are often non-specific. Although US is useful in the diagnosis of this condition, CT is the imaging technique of choice. US demonstrates an enlarged kidney with cystic areas corresponding to enlarged calyces. Characteristic CT findings include a non-functioning enlarged kidney with a staghorn calculus within a contracted renal pelvis. Expansion of calyces, parenchymal atrophy and inflammatory changes in perinephric fat are also strongly suggestive of XP. Calyces are filled with hypodense inflammatory infiltrate; these hypoattenuating calyces, with lipid content, often show around zero or negative HU values. Psoas abscess and fistula formation are the typical patterns of disease progression. Nephrectomy is the treatment of choice; percutaneous nephrostomy is not indicated. Accidental intraperitoneal seeding during surgery, as for our case, has not been previously described in the literature. Focal XP must be differentiated from other causes of hydronephrosis including obstructing urothelial carcinoma, and cystic masses such as cystic renal cell carcinoma and multilocular cystic nephroma.

Imaging Findings

Contrast-enhanced coronal and axial CT images demonstrate a non-functioning enlarged right kidney with staghorn calculi, dilated calyces and renal atrophy (Figs. 1.13 and 1.14). Contrast-enhanced axial and coronal CT scans, 6 months after surgery, demonstrate enhancing masses with hypodense center and calcifications in the omentum (Fig. 1.15) and between the uterus and bladder (Fig. 1.16). Surgery demonstrated granulomatous tissue containing lipid-laden macrophages consistent with intraperitoneal seeding of XP.

Case 5
Multiple Angiomyolipomas

A 44-year-old woman with tuberous sclerosis presented to the emergency room with sudden right flank pain, hypotension and skin pallor.

Fig. 1.17

Fig. 1.18

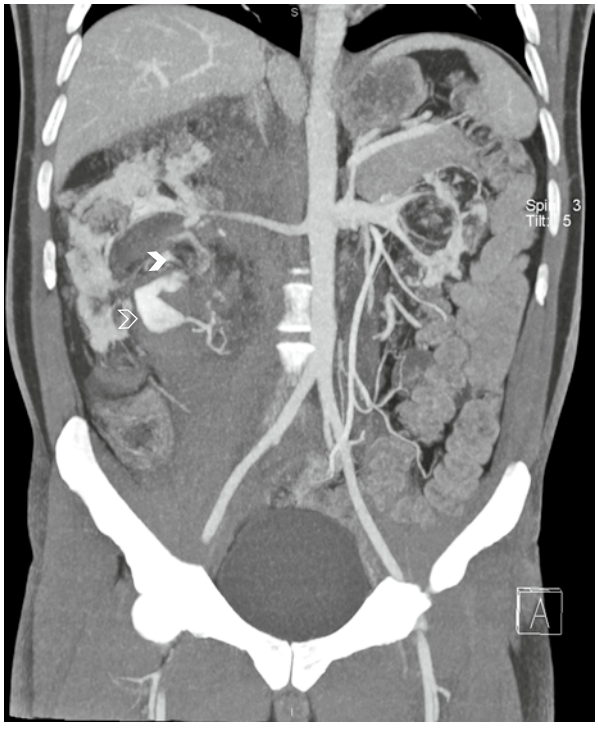

Fig. 1.19

Fig. 1.20

Comments

Angiomyolipomas are hamartomas containing varying proportions of fat, smooth muscle and thick-walled blood vessels. Epidemiologically, angiomyolipoma (AML) is seen in two distinct clinical settings. Approximately 80% of AMLs occur in middle-aged adults, with a significant female predisposition. In this population, the lesions are usually small, solitary and asymptomatic. The remaining 20% of patients with AML have tuberous sclerosis. Renal AMLs are present in approximately 80% of patients with tuberous sclerosis. AMLs in these patients are usually multiple, bilateral tumors that usually reach a large size and are often symptomatic (pain, gross hematuria, anemia, etc.). Tumors >4 cm carry an increased risk for potentially life-threatening hemorrhage (Wünderlich syndrome), which has been reported in up to 10% of these patients.

A reliable diagnosis of AML can be made based on imaging features when fat is demonstrated within a renal mass. At least 90% of AMLs contain fat that is detectable with thin-section CT or MRI. The detection of fat within a mass that arises in the kidney is considered diagnosis of AML. Other features supporting the diagnosis of AML include the presence of enlarged or aneurysmal vessels within the tumor. Isolated cases of RCC, Wilm's tumor or oncocytoma with intratumoral fat have been reported. Liposarcomas arising from the renal capsule are uncommon and may contain mature fat. Liposarcomas are rare tumors that usually occur in older patients, and are generally large at the time of diagnosis and centered in the perinephric space. These tumors displace or compress the kidney and are hypovascular without enlarged internal vessels or aneurysms.

At sonography, an AML is characteristically more echogenic than the surrounding renal parenchyma and shows an acoustic shadowing. However, this feature is also seen in 32% of small renal cell carcinoma (<3 cm in diameter). Therefore, sonography does not allow a diagnosis with the degree of confidence achieved by CT. When a small amount of fat is suspected in a renal mass, an unenhanced CT examination with thin sections and, if necessary, a pixel analysis (<−10 UH) is the most sensitive test to confirm diagnosis.

At MRI imaging, the most reliable demonstration of macroscopic fat within an AML can be achieved by comparing the appearance of the tumor on T1-weighted images with fat-saturation sequences. AMLs with a predominant fatty component are isointense relative to fat in all MRI sequences. Macroscopic fat appears bright on T1-weighted images, and the signal visible decreases with fat saturation. The use of in-phase and opposed-phase imaging is also helpful in the diagnosis of very small lesions of AML. In predominantly fatty AMLs, a characteristic India ink artifact is seen at the interface between the fat-containing mass and the normal renal parenchyma on opposed-phase, whereas the central portions of the lesion do not demonstrate changes in signal intensity in comparison with the in-phase images.

Imaging Findings

Axial unenhanced CT (Fig. 1.17) shows multiple bilateral lesions that contain fat, being compatible with AML (open arrows). Right anterior perirenal and pararenal hyperdense (36 UH) collection is suggestive of hematoma (arrow). Axial nephrographic-phase CT scan (1 mm) shows (Fig. 1.18) arterial pseudoaneurysm (open arrowhead) arising from the inferior polar branch of the right kidney with contrast extravasation (solid arrow head). Coronal MIP reconstructions (Fig. 1.19) and angiographic images (Fig. 1.20) show similar findings. The pseudoaneurysm was successfully embolized.

Case 6

Renal Lymphoma

Comments

A 69-year-old patient presented with left flank pain and fever of 2 months of duration.

Renal involvement by lymphoma may be due to hematogenous dissemination or contiguous extension of retroperitoneal disease. Renal lymphoma may also be seen in immunocompromised patients. Primary renal lymphoma that is isolated to the renal parenchyma with no systemic manifestations is uncommon (less than 1% of extranodal lymphoma).

Understanding of tumor growth and the mechanism of spread histologically is important to interpret the resulting patterns of involvement. Hematogenous involvement usually results in bilateral distribution of tumor foci within renal cortex.

Contrast-enhanced computed tomography in the nephrographic-phase imaging is the most sensitive for lesion detection. If the tumor is central and affects the hilar region or collecting system, excretory phase imaging is necessary.

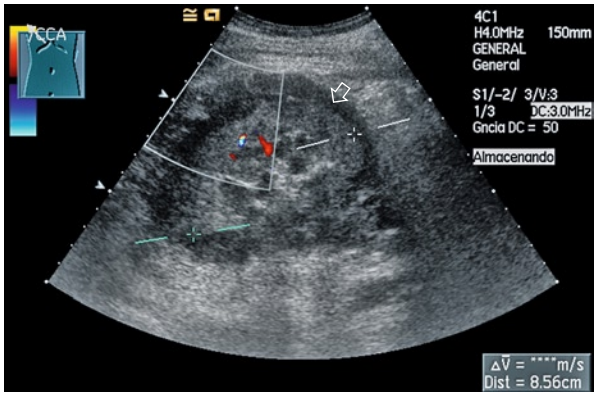

Fig. 1.21

Fig. 1.22

Fig. 1.23

Fig. 1.24

The suggestion of renal lymphoma is one of the few situations in which renal biopsy should be recommended, since the diagnosis of lymphoma determines medical therapy.

Renal lymphoma has a wide variety of CT appearances.

1. Multiple renal masses

Involvement is typically bilateral, but may also affect only one kidney. At contrast-enhanced-CT the lesions enhance less than the normal renal tissue and appear as relatively homogeneous masses. The presence of retroperitoneal adenopathy is an additional clue of the diagnosis. In MR images, minimal heterogeneous enhancement is seen on early and delayed gadolinium-enhanced MR images. At US lesions appear typically hypoechoic and homogeneous. There are benign and malignant entities that mimic renal lymphoma including metastatic disease, acute pyelonephritis, renal infarcts, abscesses and multiple synchronous renal cell carcinomas.

2. Direct extension from retroperitoneal adenopathy

The second most common presentation of renal lymphoma is as contiguous extension to the kidneys or perinephric space from large retroperitoneal masses (25–30% of cases). At CT, lymphomatous masses usually envelop the renal vasculature invading the renal hilum. However, the vasculature remains patent despite tumor encasement, a finding that is characteristic of lymphoma, and thrombosis is rare.

3. Solitary lesion

Renal lymphoma manifests as a solitary mass that grows primarily by expansion in 10–25% of patients. At contrast-enhanced-CT the masses are typically hypovascular and demonstrate minimal enhancement.

4. Perinephric disease

Isolated perinephric lymphoma is unusual (<10% of cases). The presence of a mass of perinephric soft tissue compressing the normal parenchyma without causing significant impairment of renal function strongly suggests the diagnosis although occurs infrequently.

CT in nephrographic phase is crucial for demonstrating a perirenal mass and accurate staging. At US, hypoechoic tissue of variable thickness is seen surrounding the kidney. The differential diagnoses include sarcoma arising from the renal capsule and metastases to the perinephric space, as well as benign entities such as perinephric hematoma, amyloidosis and retroperitoneal fibrosis.

Imaging Findings

US imaging (Fig. 1.21) shows hypoechoic tissue (open arrow) surrounding the left kidney. Axial CT image at nephrographic phase (Fig. 1.22) shows hypodense and homogeneous soft tissue mass (open arrow) surrounding the left kidney that enhance less than the normal renal tissue. The mass causes anterior displacement, and focal cortical infiltration of left kidney (arrowhead). The ipsilateral psoas muscle is also infiltrated (arrowhead). Small retroperitoneal lymph nodes were identified (arrowhead). Axial CT imaging at excretory phase (Fig. 1.23) shows that the mass affects collecting system produces hydronephrosis. Excretory phase image shows delayed uptake and elimination of contrast material. Axial delayed gadolinium-enhanced fat-suppressed T1-weighted sequence (Fig. 1.24) performed 1 month later shows bilateral perirenal masses (open arrows) with minimal heterogeneous enhancement that extend above the large retroperitoneal vessels (arrowhead) and infiltrate the pancreatic isthmus (arrowhead) and cortical parenchyma.

Case 7

Renal Fusion Anomaly: Horseshoe Kidney

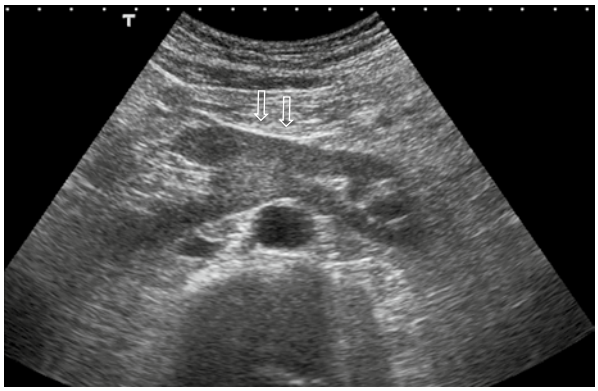

Fig. 1.25

Fig. 1.26

Fig. 1.27

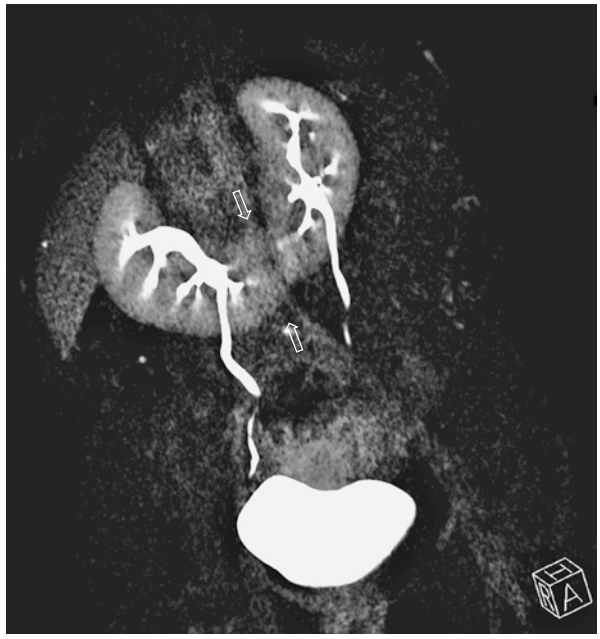

Fig. 1.28